ELSEVIER

Catalysis Today 35 (1997) 393–405

CATALYSIS TODAY

NH_3-TPD and XPS studies of Ru/Al_2O_3 catalyst and HDS activity

Masatoshi Nagai *, Kenji Koizumi, Shinzo Omi

School of Bio-applications and Systems Engineering and Department of Chemical Engineering, Tokyo University of Agriculture and Technology, Koganei, Tokyo 184, Japan

Abstract

The effects of pretreatment of catalyst on its surface properties and the HDS activity of a 0.49% Ru/Al_2O_3 catalyst were studied in a single-pass, differential microreactor. The surface properties of the catalyst were measured by NH_3-TPD and XPS analysis. The Ru/Al_2O_3 catalyst was pretreated in three ways: reduced in H_2 (Ru-R catalyst), oxidized in air and subsequently reduced in H_2 (Ru-OR catalyst), or sulfided in H_2S/H_2 (Ru-S catalyst). Three types of peaks (low, middle, and high temperatures) were observed in the NH_3-TPD study. The predominant high-temperature peak was observed for both the Ru-OR and Ru-S catalysts, pretreated at 300°C. Mass spectrometry showed that the high-temperature peak in NH_3-TPD consisted of N_2 and H_2 formed from the decomposition of NH_3 on the ruthenium sites. NO adsorption of unsaturated Ru species was related to the low-temperature peak in the NH_3-TPD. The XPS analysis showed that the peaks at 279.9 eV, 280.6 eV, and 282.5 eV were ascribed to metallic ruthenium, RuO_2, and RuO_3, respectively. The low-, middle-, and high-temperature peaks were assigned to RuO_2, acid sites on alumina, and metallic Ru, respectively. Metallic ruthenium was effective in the HDS of thiophene and the decomposition of NH_3.

Keywords: Hydrodesulphurization; Ruthenium/alumina; Temperature-programmed desorption; X-ray photoelectron spectroscopy

1. Introduction

Several studies [1–7] on the hydrodesulfurization (HDS) over unsupported transition metal sulfides yielded periodic maxima in a volcano-shaped curve, with ruthenium displaying activity greater than that of the sulfides of the classical hydroprocessing metals, such as molybdenum and tungsten. Comparable results have been observed for carbon-supported ruthenium sulfides in the HDS of thiophene [1–3,6,7] and dibenzothiophene [4,5]. Ledoux et al. [7] ascribed the high activity of RuS_2 in HDS to elements which may exhibit various possibilities of coordination with sulfur. It has also been proposed that the presence of $(S)_2^{2-}$ is favorable for the catalytic activity of the Ru catalyst [8,9]. The genesis of an active center in the RuS_2/Al_2O_3 catalysts for the HDS reaction is important in the sulfidation step. De Los Reyes et al. [3,10,11] have recently reported the importance of the sulfidation step in the absence of hydrogen in order to obtain a well sulfided, well dispersed and highly active catalyst [10]. Furthermore, Kuo et al. [1] reported that the ratio of sulfur to Ru on the catalyst surface was found to correlate well with the selectivity for the HDS

* Corresponding author.

PII S0920-5861(96)00214-3

of thiophene, but not with the presence of RuS_2 in the bulk. They also reported that surface acidity possibly played critical roles in both thiophene activity and selectivity [2], although they have not determined the surface acidity of the catalyst. The relationship between the adsorption capacities and the catalytic properties, however, significantly depends upon the preparation and pretreatment of the ruthenium precursor catalysts. These discrepancies appear to result in changing the surface composition, surface acidity, metal dispersion and electronic property of ruthenium, after the catalyst pretreatment. The effects of catalyst pretreatment on the surface properties of the Ru/Al_2O_3 catalyst, such as surface acidity and sulfur and ruthenium content by XPS analysis, and on the activities for the HDS of thiophene, are reported in this paper.

2. Experimental

2.1. Materials

The gases were subjected to the following purification treatments: He, N_2, and H_2 (Tomoe Co., 99.999%) were purified by passing each gas through the bed of a Deoxo unit to convert O_2 impurities to H_2O and a 13X molecular sieve trap. Mixed gases including air (Takachiho Co., 78.00% N_2 and 22.00% O_2), 10% H_2S in H_2 (99.999%), and 5.06% NH_3 in He (99.999%) were used without further purification. The alumina-supported sample (>200 mesh powder; Catalysis Society of Japan; JRC-A4-0.5Ru2) was prepared by impregnation of alumina in an aqueous solution of $RuCl_3 \cdot 3H_2O$.

2.2. Pretreatment of catalysts

The Ru/Al_2O_3 catalysts were pretreated in three ways prior to catalyst characterization in a microreactor.

Ru-OR catalyst: The catalyst was heated in flowing air (25 cm^3/min) at 100°C for 1h, and then raised from 100 to 400°C at a rate of 10°C/min, calcined in flowing air at the same temperature for 3h, with the gas stream switched to flowing He (15 cm^3/min). Subsequently, the catalyst was reduced in flowing H_2 (15 cm^3/min) at the desired temperature (100–400°C) for 2h, treated in flowing He at the same temperature for 1h, and cooled in flowing He to room temperature.

Ru-R catalyst: The catalyst was treated as follows: without calcination, the catalyst was heated in flowing He at 100°C for 1h, then raised, in flowing He, from 100°C to the desired temperature at a rate of 10°C/min. The gas stream was switched to H_2, attaining reduction in flowing H_2 for 2h at the same temperature, then followed by outgassing at the same temperature in flowing He for 1h. The sample was then cooled to room temperature in flowing stream of He.

Ru-S catalyst: After heating in stream of He from 100°C to the desired temperature at a rate of 10°C/min, the gas was switched to stream of 10% H_2S/H_2 (25 cm^3/min) for sulfiding at the same temperature for 3h, followed by outgassing at the same temperature in stream of He for 1h. The sample was then cooled to room temperature in stream of He.

Table 1
Nomenclature of the catalysts pretreated under various conditions

Catalysts	Pretreatment precedures		
	Oxidation	Reduction	Sulfidation
Ru-OR100	400°C, 3h	100°C, 2h	–
Ru-OR300	400°C, 3h	300°C, 2h	–
Ru-OR350	400°C, 3h	350°C, 2h	–
Ru-OR400	400°C, 3h	400°C, 2h	–
Ru-R100	–	100°C, 2h	–
Ru-R300	–	300°C, 2h	–
Ru-R400	–	400°C,2h	–
Ru-S200	–	–	200°C, 3h
Ru-S300	–	–	300°C, 3h
Ru-S400	–	–	400°C, 3h
Ru-S300(5)	–	–	300°C, 5h
Ru-S300(9)	–	–	300°C, 9h
Al-OR300	400°C,3h	300°C,2h	–
Al-R300	–	300°C,2h	–
Al-S300	–	–	300°C, 3h

The catalysts are cooled Ru-ORT, Ru-RT, Ru-ST, Al-ORT, Al-RT, and Al-ST, as shown in Table 1, where Ru and Al stand for ruthenium and alumina, respectively, and OR, R, and S denote reduction after oxidation, direct reduction, and sulfidation, respectively, and T stands for pretreatment temperature, i.e., Ru-OR300 denotes that the Ru/Al_2O_3 catalyst was oxidized at 400°C and subsequently reduced at 300°C.

2.3. HDS activity

Thiophene was introduced into the reactor by bubbling a stream of pure hydrogen at a rate of 15 cm^3/min through a thiophene saturator, maintained in an ice bath at 0°C. The reaction was conducted, using a single-pass, differential microreactor at 300°C or 400°C, in atmospheric pressure. The concentration of thiophene in the feed stream (total flow rate 20 cm^3/min) was maintained at approximately 3.2×10^{-4} mol/l by adjusting the H_2 flow rate (5 cm^3/min) through the saturator. Sampling was performed by injecting a sample from a sampling loop into the gas chromatograph for quantitatively analyzing the amount of thiophene (2% Silicon OV-17) and the products of reaction (VZ-8). The rate of HDS of thiophene is given by,

$$\text{HDS rate} = FXC_T/W,$$

where F is the total flow rate of the feed; X the fractional conversion; C_T the concentration of thiophene in the feed; and W the catalyst weight.

2.4. Temperature-programmed desorption

After the catalyst (0.2 g) was pretreated, all of the Ru/Al_2O_3 catalysts were kept in stream of He, at 100°C for 1h. The He flow was, then, replaced with a 5% NH_3/He (or 100% NO) stream (60 cm^3/min) at 100°C for 2h. The catalyst was flushed with He at 100°C for 1.5h, and the temperature was raised to 500°C in flowing He (60 cm^3/min) at a rate of 10°C/min. The concentration of NH_3 (or NO) in the exit gas was determined, using a thermal conductivity (TCD) cell or a quadrupole mass spectrometer (ULVAC Co., QMS150A). For the NH_3(or NO)-TPD measurement, the evolved gases were sampled at frequent temperature intervals (5°C) and analyzed for NH_3, N_2, H_2, and H_2O for the NH_3-TPD, and for NO and N_2O for the NO-TPD. The mass spectra were recorded at 5°C intervals, until the final temperature of 500°C was reached.

2.5. XPS measurement

XPS measurements were taken by an ESCA-850 spectrometer, operated at 8 kV and 30 mA, using Mg K_α radiation (1253.6 eV). XPS characterization of the catalysts was obtained before and after pretreatment, and after the catalysts served on-line for 8h through the HDS. Pretreated catalysts were cooled to room temperature in a stream of He, passivated in stream of $1\%O_2$/He. For preparation of XPS samples, the samples were mounted on copper plate with silver-paste. The samples in form of powder were degassed for 2h at 200°C in a vacuum oven and then for 1.5h at room temperature in the prechamber of spectrometer (10^{-6} Pa). Binding energies were referenced to Al 2p at 74.7 ± 0.2 eV. The XPS peak areas ratios were determined by integrating areas of S $2p_{1/2}$, S $2p_{3/2}$, Ru $3d_{3/2}$, and Ru $3d_{5/2}$, using a curve-fitting program stored in a computer, assuming Gaussian peak shapes, appropriate for cross sections and the spectrometer efficiency factor. The $3d_{3/2}$ component is hidden behind a C 1s peak from a hydrocarbon contaminant in the spectrometer, but the binding energies for the Ru $3d_{5/2}$ level and C 1s level did not overlap.

2.6. Ru particle size

The average diameter of the ruthenium particles was measured by the H_2 adsorption method and calculated according to Anderson [12]:

$$d_p = 101.07(DA_M.\rho N_A)^{-1},$$

where D, A_M, ρ, and N_A represent the dispersion of Ru, the surface area of one Ru atom (8.17×10^{-20} m^2/Ru atom [2]), the Ru metal density (12.3×10^6 g/m^2[13]), and Avogadro's number, respectively. The chemisorption measurement for the Ru/Al_2O_3 catalysts (0.2 g) was obtained by a pulsated-flow technique which measured the amount of irreversible H_2 adsorption by the TCD of a gas chromatograph at 25°C. Following the pretreatment, the catalysts were purged at 25°C with He (15 cm^3/min) for 30 min. One pulse of 10% H_2/He was added to the He carrier (5.0 μl H_2/pulse) at 2-min intervals until successive hydrogen peaks increased by less than 1%.

3. Results

3.1. Activity and selectivity in the HDS of thiophene

The distribution of the products of reaction in the HDS of thiophene over the Ru/Al_2O_3 catalysts is shown in Table 2. The major products, in the HDS of thiophene, were butenes and butane. Isomers of butene were formed over the Ru/Al_2O_3 catalysts: 1-butene, *trans*-2-butene, and *cis*-2-butene. Neither the 1,3-butadiene nor tetrahydrothiophene were observed when the Ru-OR and Ru-R catalysts were used. The selectivity of hydrogenation and isomerization are also shown in Table 2, for similar conversions at different reaction temperatures. The selectivity of hydrogenation is defined as the ratio of the formation rate of butane to butenes. The selectivity of hydrogenation for the Ru-OR400 and Ru-S400 catalysts were 4 times and 12 times greater than that for the Ru-OR300 and Ru-S300 catalysts, respectively. This result indicated that the Ru/Al_2O_3 catalysts, treated at 400°C, were more selective than those treated at 300°C, during the hydrogenation of butenes to butane. Furthermore, since the ratio of 1-butene to 2-butenes represents the selectivity of isomerization for the Ru/Al_2O_3 catalyst, the Ru-S300 catalyst showed the lowest selectivity during the isomerization. The Ru-S300 was the most active in the HDS of thiophene but it was less selective than the three catalysts during both hydrogenation and isomerization. The Ru-S300 was highly selective in the breaking of the C–S bond in thiophene.

All of the Ru/Al_2O_3 catalysts treated at 300°C were more active than those at 400°C. In Table 3, the Ru-S300 catalyst was the most active of all the catalysts and was 1.4 and 3.7 times greater than that of the Ru-OR300 and Ru-R300 catalysts, respectively. Sulfidation at 300°C maximized the HDS activity of the

Table 2
Product distribution and selectivity during the HDS of thiophene on Ru/Al_2O_3 catalysts

Catalyst	Conversion (%)	Product distribution (%)					Selectivity (−)	
		Butane	Butenes			Butadiene	1-b/2-b [f]	Butane/Butenes [g] $\times 10^{-2}$
			[b]1-b [c]	t-2 [d]	c-2 [e]			
Ru-OR300	19.3 [a]	5.4	36.5	35.2	22.9	0	0.63	5.6
Ru-OR400	14.6 [b]	19.2	39.8	24.0	17.0	0	0.97	23.8
Ru-S300	11.6 [a]	3.2	21.3	44.6	30.9	0	0.28	3.3
Ru-S400	8.8 [b]	26.6	30.8	21.5	15.6	5.5	0.83	39.2

[a] Reaction temperature: 300°C.
[b] Reaction temperature: 400°C.
[c] 1-butene.
[d] *trans*-2-butene.
[e] *cis*-2-butene.
[f] The ratio of 1-butene to 2-butenes.
[g] The ratio of butane to butenes.

Ru/Al_2O_3 catalysts. The rate of the HDS of thiophene over the Ru-S400 catalyst drastically dropped to 17% of the rate of HDS over the Ru-S300 catalyst. The Ru-S catalyst was more active than the Ru-OR catalyst, except for the Ru-S400 catalyst.

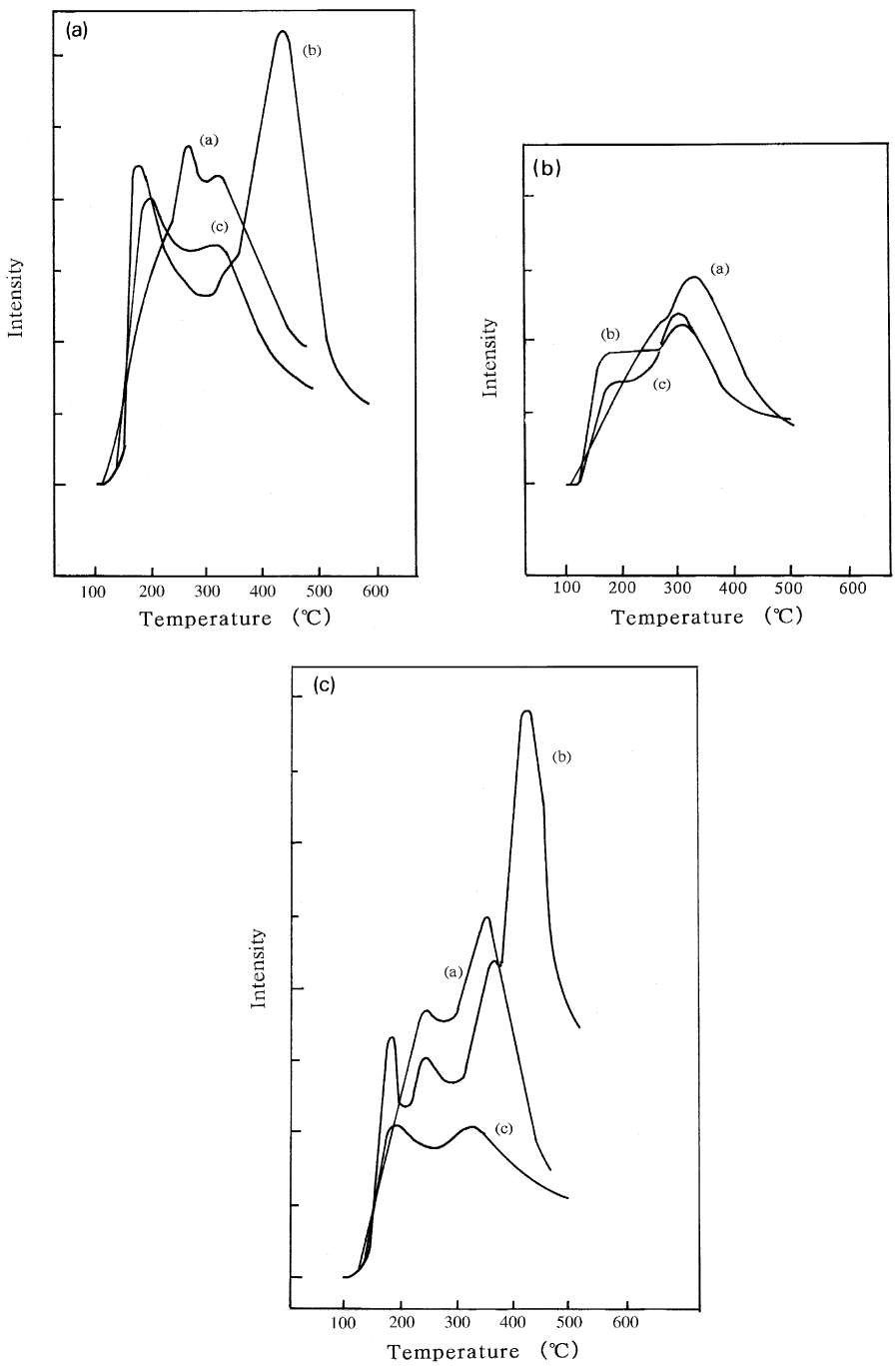

Fig. 1. A. NH_3-TPD profile for the Ru-OR and A1-OR300 catalysts: (a) A1-OR300, (b) Ru-OR300, and (c) Ru-OR400; B. NH_3-TPD profile for the Ru-R and A1-R300 catalysts: (a) A1-R300, (b) Ru-R300, and (c) Ru-R400; C. NH_3-TPD profile for the Ru-S and Al-S300 catalysts: (a) Al-S300, (b) Ru-S300, and (c) Ru-S400.

3.2. NH_3-TPD

NH_3-TPD profiles for the Ru/Al_2O_3 catalysts under three different pretreatment conditions are shown in Fig. 1: Fig. 1A for Ru-OR, Fig. 1B for Ru-R, and Fig. 1C for Ru-S. With the Ru-OR catalysts, the desorptgrams showed two well resolved peaks with small middle-temperature ones at 167–192°C and at 425–450°C, and at 321–334°C. This result indicated that three types of adsorption sites for NH_3 were present on the Ru-OR catalysts. The sulfided catalyst, Ru-S catalyst, is similar to the Ru-OR catalyst in NH_3-TPD profile. The Ru-S300 catalyst has a remarkable high-temperature peak with small low-temperature peaks, whereas the Ru-S400 catalyst has no high-temperature peaks, as shown in Fig. 1C. Thus, both the Ru-OR300 and Ru-S300 catalysts have a marked high-temperature peak. No high- and low-temperature peaks but middle-temperature ones were observed for alumina treated under the same pretreatment conditions. The middle-temperature peak for the Ru-OR300 and Ru-OR400 catalysts was ambiguous and smaller than that for the alumina alone. Since the middle-temperature peak was observed for all alumina with three kinds of treatment, the peak was due to the release of NH_3 from alumina. Consequently, the low- and high-temperature peaks are due to the presence of two types of ruthenium species on the surface of the Ru/Al_2O_3 catalysts. The middle-temperature peak for Al-OR300 was larger than those of the Ru-OR300 and Ru-R300 catalysts. If ruthenium covered the alumina sur-

Table 3
Ru Particles of the Ru/Al_2O_3 catalyst and HDS rate

Catalyst	Ru particle size [a] [nm]	HDS rate [b] [μmol/s·g]
Ru-OR100	12.3	0.0896
Ru-OR300	2.6	0.200
Ru-OR350	4.4	0.114
Ru-OR400	7.6	0.0779
Ru-R100	26.7	0.0539
Ru-R300	14.5	0.0741
Ru-R400	22.9	0.0261
Ru-S200	3.0	0.191
Ru-S300	2.0	0.275
Ru-S400	26.6	0.0469

[a] Ru particle size measured by H_2 uptake measured by pulse chemisorption at 25°C.
[b] Reaction temperature, 400°C.

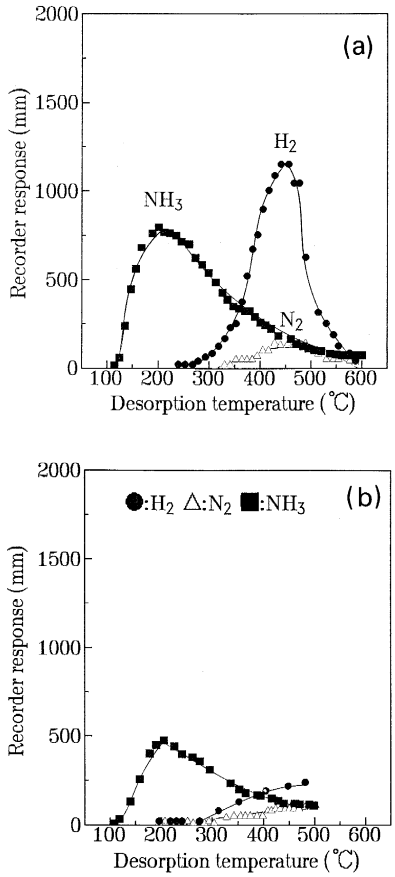

Fig. 2. NH_3-TPD spectra from mass spectroscopy for the Ru-OR300 catalyst (A) and the Ru-R300 catalyst (B).

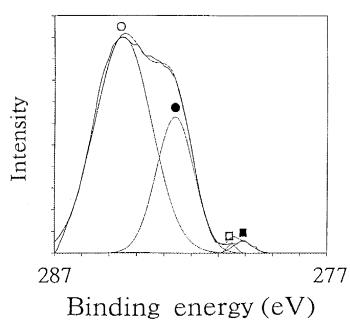

Fig. 3. Ru $3d_{2/5,3/2}$ and C 1s XPS of the Ru-OR400 catalyst. ○: C, ●: RuO_3, □: RuO_2, ■: Ru^0.

face after pretreatment, the middle-temperature peak of NH_3 originated by Al_2O_3 was probably reduced and shifted to the low-temperature peak by the Ru species. The Ru-R catalysts displayed no significant high-temperature peak but only middle- and small low-temperature peaks, as shown in Fig. 1B, suggesting that the directly reduced catalysts had the surface acidity of alumina and the ruthenium species derived from the low-temperature peak.

In order to determine what kind of gases were released from the catalyst during the NH_3-TPD, the spectra from mass spectroscopy of the Ru-OR300 and Ru-R300 catalysts are shown in Fig. 2A and Fig. 2B. For the Ru-OR300 catalyst, ammonia is gradually released starting at 100°C, reaching a maximum at 200°C and then decreased with desorption temperature, but N_2 and H_2 gases were detected in the high-temperature region. On the contrary, for the Ru-R300 catalyst, N_2 and H_2 were barely formed in the high-temperature region as shown in Fig. 2B. From the results, two types of ruthenium species are present on the surface: the one species is active during the decomposition of NH_3 to form N_2 and H_2, and the other is an acid site on which ammonia is adsorbed.

3.3. Ru species

A typical Ru $3d_{5/2}$ XPS spectrum for the pretreated Ru/Al_2O_3 catalysts is shown Fig. 3.

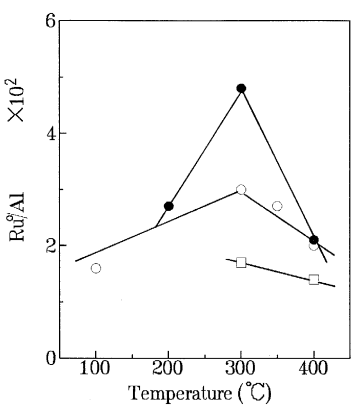

Fig. 4. The XPS atomic ratio of Ru^0 3d XPS to Al 2p of the Ru/Al_2O_3 catalysts versus pretreatment temperatures. ●: Ru-S, ○: Ru-OR, □: Ru-R.

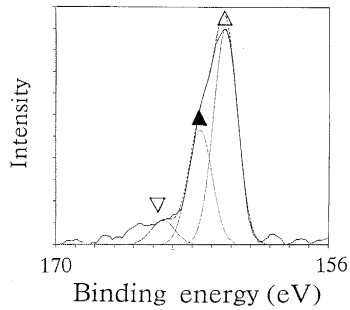

Fig. 5. S $2p_{1/2,3/2}$ XPS of the Ru-S400 catalyst. △: S^{2-}, ▲: $(S_2)^{2-}$, ▽: S^0.

The Ru $3d_{5/2}$ binding energies at 279.9, 280.7 and 282.5 eV were observed for all of the catalysts. The binding energy at 279.9 eV agrees quite well with the binding energy reported for Ru^0 metal [10,14,15]. The Ru $3d_{5/2}$ binding energy at 280.7 eV was in agreement with the reported value (281.0 eV) for RuO_2, as reported by Pedersen and Lunsford [16]. The binding energies of Ru $3d_{5/2}$ was reported 280.8 eV and 282.5 eV for RuO_2 and RuO_3, respectively [15]. The peaks at 279.9, 280.7, and 282.5 eV were, consequently, ascribed to metallic Ru (Ru^0), RuO_2 and RuO_3, respectively. For the Ru-S catalysts, ruthenium disulfide is possibly formed, as well as Ru metal, during sulfidation of the Ru/Al_2O_3 catalyst. The XPS binding energy (i.e., Ru $3d_{5/2}$ at 280.8 eV) of Ru^{4+} ion in RuO_2 is quite close to those of Ru^{2+} in ruthenium disulfide (280.4 eV) [10,17].

The atomic ratio of Ru $3d_{5/2}$ (Ru^0; 279.9 ± 0.4 eV) to Al 2p versus pretreatment temperature of the Ru/Al_2O_3 catalysts is shown in Fig. 4. The atomic ratio of Ru/Al showed a maximum at the pretreatment temperature of 300°C for three different types of catalysts. The Ru-S300 catalyst had the highest ratio of Ru^0/Al compared to the other catalysts. Furthermore, there were no relationships among treatment temperature and the atomic ratio of the RuO_2/Al and RuO_3/Al peak areas. The data, therefore, showed that the Ru^0 metal was exposed on the surface of the Ru-S300 catalyst, compared to the other catalysts.

3.4. Sulfur species

A typical S 2p XPS spectrum for the Ru-S300 catalyst is shown in Fig. 5. The XPS binding energies at 161.3, 162.7, and 164.4 eV were observed for the Ru-S catalysts. A weak shoulder peak was found at 164.4 eV, suggesting the presence of elemental sulfur, e.g., S^0, at the surface, although the peak at 164.4 eV was covered with noise. The two XPS binding energies at 161.3 and 164.5 eV were reported for the S^{2-} and S^0 ions by Cocco and Tatarchuk [18]. The binding energy at 162.7 eV was also characteristic of disulfide polyanions $(S_2)^{2-}$, as previously reported by De Los Reyes [3,10,11]. This value was close to the characteristic bond of the bulk RuS_2 which had a pyrite structure (162.5 eV) [3,15]. The Ru-S catalyst contained metallic ruthenium, as well as ruthenium disulfide.

3.5. Ru and sulfur contents

The atomic ratios of S $2p_{1/2,3/2}$/Ru $3d_{5/2}$ and S $2p_{1/2,3/2}$/Al 2p of the Ru/Al_2O_3 catalysts, those before and after the reaction, are shown in Table 4. The Ru-OR400, Ru-S300, and Ru-R400 before reaction had greater ratios of total Ru/Al and RuO_3/Al but only Ru-S300 had a Ru^0/Al greater than those of other catalysts. This result suggested that Ru^0 metal was highly dispersed as Ru^0 metal on the surface of the Ru-S300 catalyst. On the other hand, the total Ru/Al ratios were small for the Ru-OR300, Ru-R300, and Ru-S400 catalysts. The ratio of Ru^0/Al for Ru-OR300 was relatively greater than that of Ru-R300 and Ru-S400. These results implied that Ru^0 metal on the surface was related to the HDS activity of Ru/Al_2O_3 catalysts, in combination with the data for the rate of HDS of thiophene. The greater Ru/Al atomic

Table 4
XPS data for Ru/Al_2O_3 catalysts

Catalyst	Ru/Al [a], Ru content $\times 10^2$				S/Al [b], sulfur content $\times 10^2$			
	RuO_3 [e]	RuO_2 [f]	Ru^0 [g]	total	S^{2-} [h]	$(S_2)^{2-}$ [i]	S^0 [j]	total
Ru-OR300 BR [c]	1.7	0.6	3.0	5.3	–	–	–	–
Ru-OR300 AR [d]	9.1	0.2	1.3	10.6	1.2	1.9	1.8	4.9
Ru-OR400 BR	14.4	0.3	2.0	16.7	–	–	–	–
Ru-OR400 AR	16.9	0	0	16.9	0.4	0.5	0.4	1.4
Ru-R300 BR	3.0	0.4	1.7	5.1	–	–	–	–
Ru-R300 AR	5.5	0	2.2	7.8	0.8	0.4	0.4	1.5
Ru-R400 BR	14.0	0.4	1.4	15.9	–	–	–	–
Ru-R400 AR	21.6	0	0	21.6	0.3	0.4	0.6	1.2
Ru-S200 BR	10.4	0.3	2.7	13.4	1.9	3.3	3.7	8.9
Ru-S300 BR	9.0	0.3	4.8	14.1	1.7	3.2	5.8	10.7
Ru-S300 AR	12.8	0.2	5.5	18.4	1.3	1.3	0.8	3.3
Ru-S400 BR	2.7	0.3	2.1	5.1	18.5	6.7	1.6	26.7
Ru-S400 AR	3.0	0.8	3.8	7.6	1.5	2.0	2.8	6.3
Ru-S300(5) [k] BR	8.9	4.6	1.9	15.4	7.8	4.7	3.8	16.3
Ru-S300(9) [k] BR	10.7	1.9	0.2	12.9	21.1	13.3	2.3	36.8

[a] The atomic ratio of Ru 3d/Al 2p measured using XPS.
[b] The atomic ratio of S $2p_{1/2,3/2}$/Al 2p measured using XPS.
[c, d] BR and AR stand for before and after reaction, respectively.
[e] Ru $3d_{3/2}$, 282.5 ± 0.6 eV [15,16].
[f] Ru $3d_{5/2}$, 280.6 ± 0.4 eV (RuO_2); 280.4 ± 0.4 eV (RuS_2) [10,17].
[g] Ru $3d_{5/2}$, 279.9 ± 0.4 eV [10,14,15].
[h] S $2p_{3/2}$, 161.3 ± 0.2 eV (161.3 eV, [17]).
[i] S $2p_{3/2}$, 162.7 ± 0.2 eV (162.5, [3]; 163.1 [15]).
[j] S $2p_{3/2}$, 164.4 ± 0.2 eV (164.5 eV [18]).
[k] Indicates sulfiding time (5h or 9h) in parentheses. No parentheses indicate 3 h.

ratio for the Ru-S catalysts corresponded to a high rate for the HDS of thiophene.

As shown in Table 4, the S^{2-}/Al and the $(S_2)^{2-}/Al$ of Ru-S400 (BR) greater than those of Ru-200 and Ru-300 (BR), but the total S/Al attained a maximum at a sulfidation temperature of 300°C. The maximum Ru/Al atomic ratio of Ru-S300 (BR) is considered to be related to S^0 but not $(S_2)^{2-}$ and S^{2-}, suggesting the formation of metallic ruthenium. The contents of the total S/Al, S^{2-}/Al, and $(S_2)^{2-}/Al$ of the Ru-S (BR) catalysts substantially increased with protracted sulfiding time, but the S^0/Al species decreased. Thus, severe sulfiding treatment generated sulfide ions, S^{2-}, and disulfide polyanions, $(S_2)^{2-}$, indicating the formation of RuS and RuS_2 on the surfaces of the catalysts. The tendency of the S^0/Al toward the sulfiding temperature was described with a volcano-type curve having a maximum at a pretreatment temperature of 300°C.

As for the catalysts after reaction, the Ru-OR300 (AR) catalyst held a greater total S/Al ratio than the Ru-OR400 (AR) catalyst, but the Ru-R catalysts displayed small values. The total S/Al ratio of the catalyst (AR) reflected HDS activity of the Ru/Al_2O_3 catalysts. The Ru-OR and Ru-R (AR) catalysts were partially sulfided and sulfur deposited from the scission of the C–S bond of thiophene during the reaction. For the Ru-S catalyst, the total S/Al ratio decreased after the reaction. These results show that the surface was possibly changed in flowing H_2 during the reaction, causing the increase in Ru/Al atomic ratio and the decrease in total S/Al ratio.

3.6. NO-TPD

NO desorbed together with a very small amount of N_2O during NO-TPD adsorbed NO for 2h at 100°C, as shown in Fig. 6. No desorption of N_2 gas was observed in NO-TPD, suggesting there was no reaction of NO on Ru to form N_2 and O_2. The data suggested that almost all NO adsorbed on the catalyst surface were

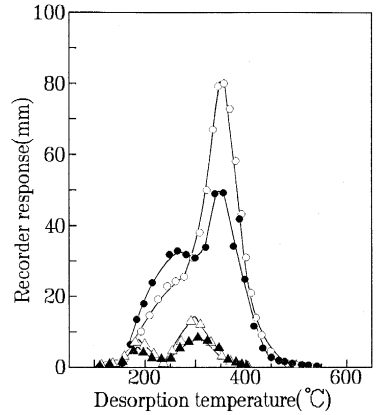

Fig. 6. NO adsorption for the Ru/Al_2O_3 catalysts at 100°C. ○: Ru−OR300, ●: Ru-OR400, △: Ru-S300, ▲: Ru-S400.

desorbed unchanged from the catalyst. The NO-TPD profile displayed a main peak at about 350°C with a shoulder peak at about 250°C, as shown in Fig. 6. Uchida and Bell [19] studied NO adsorption on 5% Ru/Al_2O_3 reduced in H_2 at 450°C, in flowing NO for 30 min at 100°C and reported two NO peaks in the range of 100 to 450°C. The high-temperature peak in the NO-TPD desorptgram for the Ru-OR300 was higher than that for the Ru-OR400, while the low-temperature peak for the Ru-OR400 was higher. This is probably due to high reduction of the Ru atom of the catalyst. The Ru-S300 and Ru-S400 catalysts displayed almost similar, small broad peaks in the NO-TPD desorptgram. Since the Ru-OR300 catalyst was more active than the Ru-OR400 and Ru-R catalysts, the high-temperature peak in the NO-TPD was related to the rate of the HDS of thiophene. The results of the NO-TPD study suggested that the Ru-OR catalyst had a higher number of unsaturated Mo sites on the surface. For the Ru-S catalysts, however, two desorption peaks were smaller, 50–70°C lower than those for the Ru-OR catalysts. NO was adsorbed on Ru^0 and Ru^{2+} surface sites present on the reduced catalyst [20]. The two peaks were due to NO adsorption on Ru^0 and Ru^{2+} on the surface. However, the two smaller Ru-S catalysts displayed greater high-temperature desorption peaks than

the Ru-OR catalysts. New types of Mo unsaturated sites were probably produced, consequently, on the Ru-S catalysts, which were different from the sites on the Ru-OR and Ru-R catalysts. Although the Ru-S300 catalyst was more active than the Ru-OR catalyst during the HDS of thiophene, the Ru-S300 held lower NO uptakes than the Ru-OR catalysts. As a result, therefore, Ru unsaturated sites are unlikely to be effective in the HDS of thiophene.

3.7. Ru particle size

The particle size of Ru in the Ru/Al_2O_3 catalysts are given in Table 3. The particle size of Ru of the catalysts pretreated at 400°C in flowing H_2 or 10% H_2S/H_2 were larger than those pretreated at 300°C. The Ru-R catalyst had larger Ru particles than the Ru-OR catalyst. The particle size of Ru was very small for the Ru-S300 catalyst. A sulfidation temperature from 300 to 400°C decreased the particle size of Ru of the Ru-S catalyst from 2.0 nm to 26.6 nm, respectively.

4. Discussion

4.1. Ru and S contents and the HDS of thiophene

The ratio of the Ru 3d/Al 2p peak and both peak areas of NH_3-TPD, at low and high temperature, were described with a volcano-type curve having a maximum at the pretreatment temperature of 300°C. The ratio of the XPS $Ru(RuO_2)/Al$ is plotted against the amount of released NH_3 (surface acidity) in the low-temperature peak of NH_3-TPD, as shown in Fig. 7. Since the area of NH_3 released from the low-temperature region agreed with the number of RuO_2 sites on the Ru/Al_2O_3 catalyst, the surface acidity of the Ru/Al_2O_3 catalyst was generated on RuO_2. The area of the high temperature in NH_3-TPD is also related to the ratio of $Ru(Ru^0)/Al$, as shown in Fig. 8. The area of

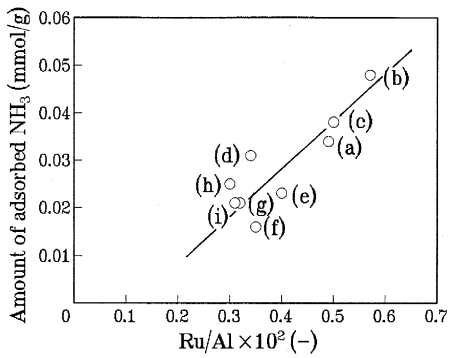

Fig. 7. Relationship between the ratio of the XPS $Ru(RuO_2)/Al$ 2p peak area and the amount of adsorbed NH_3. The amount of adsorbed NH_3 was calculated from the peak area which was determined by an integration of the desorption temperature versus intensity in NH_3-TPD: (a) Ru-OR100, (b) Ru-OR300, (c) Ru-OR350, (d) Ru-OR400, (e) Ru-R300, (f) Ru-R400, (g) Ru-S200, (h) Ru-S300, (i) Ru-S400.

NH_3-TPD at high temperature consisted of N_2 and H_2 gases formed from the decomposition of NH_3. The high-temperature peak, therefore, was related to metallic Ru species, on which the decomposition of NH_3 took place, while the low-temperature peak was related to RuO_2. Metallic ruthenium on the surface of the Ru/Al_2O_3 catalysts facilitated the decomposition of NH_3.

The rate of the HDS of thiophene is plotted versus the S/Al atomic ratio before reaction, as shown in Fig. 9. The rate of the HDS of thiophene drastically decreased with increasing ratios of $(S_2)^{2-}/Al$ and S^{2-}/Al, and conse-

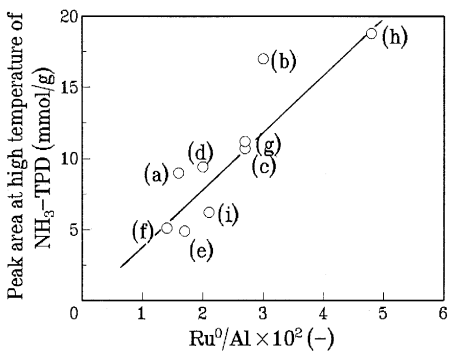

Fig. 8. Relationship between the atomic ratio of the XPS Ru (Ru^0)/Al 2p and the amount of evolved gases in high-temperature region of the NH_3-TPD. See the symbols in Fig. 7.

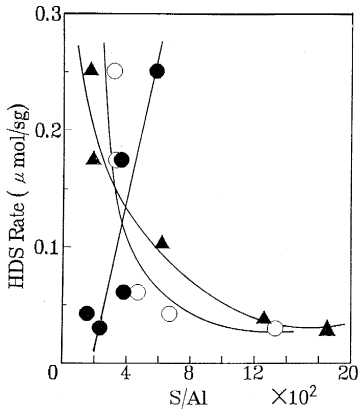

Fig. 9. Effect of the S 2p/Ru $3d_{5/2}$ atomic ratio before reaction on the HDS activity of the Ru-S catalyst. ▲: S^{2-}/Ru, ○: $(S_2)^{2-}$/Ru, ●: S^0/Ru.

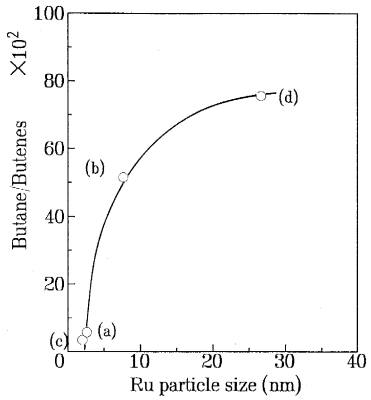

Fig. 11. Influence of Ru particle size on hydrogenation selectivity: (a) Ru-OR300, (b) Ru-OR400, (c) Ru-S300, and (d) Ru-S400.

quently the activity of the Ru/Al_2O_3 catalyst quickly decreased with sulfiding of the ruthenium atom. The rate of the HDS of thiophene was proportional to the ratio of S^0/Al. This result suggested that the HDS activity of the catalysts did not depend on $(S_2)^{2-}$ and S^{2-} ions but on the elemental S^0 content for total Ru on the catalysts. Since the increased content of $(S_2)^{2-}$ and S^{2-} ions decreased the HDS activity of the catalyst, sulfidation of the Ru atom to RuS or RuS_2 [17] reduced the activity of the Ru/Al_2O_3 catalysts. This result was in agreement with the study that showed an extensive sulfidation using 100% H_2S at 400°C for 2h resulted in decreased HDS activity of the catalyst, attributed to the formation of crystalline RuS_2 on the surface [21]. Lacroix et al. [22] reported that catalytic activities for the reactions of H_2–D_2 exchange and 1-butene hydrogenation did not correlate with the concentration of $(S_2)^{2-}$ pair anions but did correlate for the coordinatively unsaturated ruthenium cation, by partial reduction of RuS_2. The activity of the Ru/Al_2O_3 catalyst is thus decreased by sulfidation of ruthenium to form RuS_2. The rate of the HDS of thiophene as a function of the atomic ratio of Ru $3d_{5/2}(Ru^0)/Al$ 2p for the Ru/Al_2O_3 catalysts before the reaction is shown in Fig. 10. The rate of the HDS of thiophene for the Ru/Al_2O_3 catalysts was proportional to the Ru^0/Al ratio. There was no relationship between the HDS of thiophene and the contents of RuO_2 and RuO_3 of the Ru/Al_2O_3 catalysts. The HDS activity of the Ru/Al_2O_3 catalysts, therefore, depended on the Ru^0 metal on the catalyst surface.

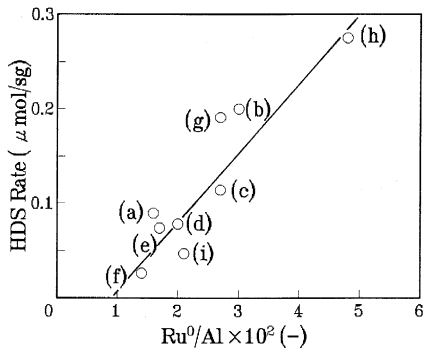

Fig. 10. Relationship between the atomic ratio of Ru^0/Al and the activity of the Ru/Al_2O_3 catalyst during the HDS of thiophene: (a) Ru-OR100, (b) Ru-OR300, (c) Ru-OR350, (d) Ru-OR400, (e) Ru-R300, (f) Ru-R400, (g) Ru-S200, (h) Ru-S300, (i) Ru-S400.

4.2. Effects of particle size on hydrogenation selectivity

The selectivity of hydrogenation in relation to Ru particle size for the Ru-OR and Ru-S catalysts is shown in Fig. 11. The selectivity of hydrogenation increased with increasing Ru particle size of the catalysts. The selectivity of

hydrogenation for the Ru-S400 catalyst with large Ru particles was significantly higher than that for the Ru-S300 catalyst with small Ru particles. Lu et al. [21] reported the H_2–D_2 exchange rate at 300°C over extensively sulfided ruthenium sponge (sulfidation with 100% H_2S at 400°C for 2h) to be ca. two orders of magnitude greater than those over mildly sulfided catalysts (10% H_2S/H_2 at 400°C for 2h). The rate of the hydrogenation of thiophene, thus increased with increasing Ru crystallite size, compared to the C–S bond cleavage of thiophene during the HDS of thiophene. Heise et al. [23] reported that coordinatively unsaturated S–S anion pairs located on the surface of the RuS_2 catalysts were sites for hydrogen adsorption in the form of sulfhydryl groups (S–H), leading to the enhancement of hydrogenation. Furthermore, an extensive sulfidation at higher H_2S/H_2 ratios produced RuS_2-like surfaces, which contributed to the higher activity for hydrogenation, attributed to the formation of $(S_2)^{2-}$ anion pairs at the surface of the catalyst. Cocco and Tatarchuk [18] also suggested that an extensive sulfidation in 100% H_2S facilitated the formation of $(S_2)^{2-}$ anions, resulting in the formation of isolated S_2H_2 groups, which possibly contribute to the high hydrogenation activity.

Concerning the Ru-OR catalysts, the Ru-OR400 catalyst with a Ru particle size of 7.6 nm had higher selectivity for hydrogenation as compared to the Ru-OR300 catalyst with a Ru particle size of 2.6 nm. This observation was in agreement with the results of the Fisher–Tropsch reaction over ruthenium catalysts in that the hydrogenation of CO increased with increasing Ru particle size [24–27]. The number of hydrogenation sites, thus, rapidly increased with increasing Ru particle size.

As shown in Table 3, the HDS of thiophene over the Ru-S300 catalyst with a 2 nm particle size was 5.9 times greater than that over the Ru-S400 catalyst (26.6 nm). Somorjai and Blankely [28] suggested that sulfur preferentially blocked low coordination sites. H_2S preferentially dissociates on Ru surfaces with a higher density of defect-like sites with a higher dispersion [18,29]. Small Ru particles have more edges, corners, and other defect-like sites. The catalysts with small Ru particles significantly retained more HDS activity than those with larger particles. As a result, the Ru/Al_2O_3 catalyst with smaller Ru particle size was comparatively more active during the HDS of thiophene.

5. Conclusions

Three types of desorption peaks were observed in the NH_3-TPD profile. The high-temperature peak consisted of N_2 and H_2 gases from the decomposition of NH_3. The middle-temperature peak was due to release of NH_3 desorbed from alumina. The low-temperature peak contained NH_3 gas desorbed from the surface. The high-temperature peak was related to the metallic Ru species on which the decomposition of NH_3 took place. The low temperature peaks were attributed to the presence of RuO_2 species on the surface of the Ru/Al_2O_3 catalyst. The HDS activity was increased with decreasing amounts of $(S_2)^{2-}$ and S^{2-} ions but increasing the element S^0 content. There was no relationship between the HDS of thiophene and the contents of RuO_2 and RuO_3 of the Ru/Al_2O_3 catalysts. The HDS activity of the Ru/Al_2O_3 catalysts depended on the metallic Ru on the catalyst surface. The number of hydrogenation sites increased with increasing Ru particle size. The Ru/Al_2O_3 catalyst, with Ru of smaller particle size, was more active during the HDS of thiophene.

Acknowledgements

The authors are grateful to the Catalyst Reference Committee of the Catalysis Society of Japan for providing the 0.49% Ru/Al_2O_3 catalyst.

References

[1] Y.-J. Kuo, R.A. Cocco and B.J. Tatarchuk, J. Catal., 112 (1988) 250.
[2] Y.-J. Kuo and B.J. Tatarchuk, J. Catal., 112 (1988) 229.
[3] J.A. De Los Reyes, M. Vrinat, C. Geantet and M. Breysse, Catal. Today, 10 (1991) 645.
[4] T.A. Pecoraro and R.R. Chianelli, J. Catal., 67 (1981) 430.
[5] M. Lacroix, N. Boutarfa, C. Guillard, M. Vrinat and M. Breysse, J. Catal., 120 (1989) 473.
[6] J.P.R. Vissers, C.K. Groot, E.M. van Oers, V.H.J. de Beer and R. Prins, Bull. Soc. Chim. Belg., 93 (1984) 813.
[7] M.J. Ledoux, O. Michaux, G. Agostini and P. Panissod, J. Catal., 102 (1986) 275.
[8] J.B. Goodenough, in M.F. Barry and P.C.H. Mitchell (Editors), Proc. 4th Int. Conf. on Chemistry and Uses of Molybdenum, Climax Molybdenum Co., Golden, CO, 1982, p. 19.
[9] C.J. Casewit and M.R. Dubois, J. Amer. Chem. Soc., 108 (1985) 5482.
[10] J.A. De Los Reyes, S. Gobilos, M. Vrinat and M. Breysse, Catal. Lett., 5 (1990) 17.
[11] J.A. De Los Reyes, M. Vrinat, C. Geantet, M. Breysse and J.G. Grimblot, J. Catal., 142 (1993) 455.
[12] J.R. Anderson, Structure of Metallic Catalysts, New York, Academic Press, 1975.
[13] Chemical Society of Japan. Chemical Handbook I (Kagaku Binran I) Ch. 3, Maruzen, 1975.
[14] G.-D. Lei and L. Kevan, J. Phys. Chem., 95 (1991) 4506.
[15] P.C.H. Mitchell, C.E. Scott, J. Bonnelle and J.G. Grimblot, J. Catal., 107 (1987) 482.
[16] L.A. Pedersen and J.H. Lunsford, J. Catal., 61 (1980) 39.
[17] M. Vrinat, M. Lacroix, M. Breysse, A. Bellaloui, L. Mosoni and M. Roubin, in M.J. Phillips and M. Ternan (Editors), Proc. 9th Int. Congress on Catalysis, Calgary, 1988, Vol. 1, p. 88. Chem. Inst. of Canada, Ottawa, 1988.
[18] R.A. Cocco and B.J. Tatarchuk, Langmuir, 5 (1989) 1309.
[19] M. Uchida and A.T. Bell, J. Catal., 60 (1979) 204.
[20] E. Gulielminotti and F. Boccuzzi, J. Catal., 141 (1993) 486.
[21] K. Lu, Y.-J. Kuo and B.J. Tatarchuk, J. Catal., 116 (1989) 373.
[22] M. Lacroix, C. Mirodatos, M. Breysse, T. Decamp and S. Yuan, in L. Guczi et al. (Editors), Proc. 10th Int. Congress on Catalysis, Budapest, 1992, Vol. A, Elsevier Science B.V., Amsterdam, 1993, p. 598.
[23] W.H. Heise, K. Lu, Y.J. Kuo, T.J. Udovic, J.J. Rush and B.J. Tatarchuk, J. Phys. Chem., 92 (1988) 5184.
[24] A. Sayari, H.T. Wang and J.G. Goodwin, Jr., J. Catal., 93 (1985) 368.
[25] C.S. Keller and A.T. Bell, J. Catal., 75 (1982) 251.
[26] D.L. King, J. Catal., 51 (1978) 368.
[27] M.D. Cisneros and J.H. Lunsford, J. Catal., 141 (1993) 191.
[28] G.S. Somorjai, D.W. Blakely and F. Zaera, J. Phys. Chem., 86 (1982) 3070.
[29] S. Bhatia, B.C. Gerstein and T.S. King, J. Catal., 134 (1992) 572.